Hindawi
Mathematical Problems in Engineering
Volume 2019, Article ID 1781427, 16 pages
https://doi.org/10.1155/2019/1781427

Research Article

Research on Indentation Rolling Resistance Based on Viscoelasticity of Cover Rubber under a Conveyor Belt

Xiaoxia Zhao[1,2] **Wenjun Meng**[1,2] **and Lidong Zhou**[1,2]

[1]*School of Mechanical Engineering, Taiyuan University of Science and Technology, Taiyuan 030024, China*
[2]*Key Laboratory of Intelligent Logistics Equipment in Shanxi Province, Taiyuan University of Science and Technology, Taiyuan 030024, China*

Correspondence should be addressed to Wenjun Meng; tyustmwj@126.com

Received 8 December 2018; Revised 11 January 2019; Accepted 20 January 2019; Published 10 February 2019

Academic Editor: Gregory Chagnon

Minimizing the power consumption of the belt conveyor is the common wish of all enterprises and even countries. Among all the resistances generated by the belt conveyor during the operation, the indentation rolling resistance accounts for the largest proportion and the power consumed is the largest. Therefore, accurately predicting and reducing the rolling resistance of indentation is the focus of current research. Firstly, based on the three-element Maxwell solid model, the dynamic loading experiments of cylindrical rubber made of conveyor belt cover material were carried out at different temperatures. The identification models of elastic moduli E_2 and E_3 and viscosity coefficient η_2 in the three-element Maxwell model were obtained, and then the fitting functions of the three parameters were gotten, which can intuitively reflect the influence of temperature. Secondly, the mathematical model of the indentation rolling resistance was derived. The mathematical model is characterized by the direct parameters such as belt speed v, thickness of backing material h, the idler radius R, and the rubber viscoelastic parameters E_2, E_3, and η_2 and the indirect parameters such as normal force P and temperature T. Afterwards, the effects of belt speed, normal force, temperature, idler radius, and thickness of underlay on the indentation rolling resistance were studied under different working conditions. After that, experimental testing and analysis were fulfilled using test equipment and compared with theoretical analysis results. The results prove that the theoretical results are basically consistent with the experimental results, in line with the actual engineering rules. Finally, the application of the results in practical engineering was analyzed superficially.

1. Introduction

Belt conveyor is one of the most economical ways to transport bulk materials in many fields such as ports and mines. With the development of the times, energy conservation has become the primary goal of belt conveyors [1]. The main resistances generated during the stable operation of the belt conveyor include the indentation rolling resistance (IRR), the running resistance of the idler, the material collision resistance, and the bending resistance of the conveyor belt [2]. The indentation rolling resistance is the largest, and the energy consumed by it accounts for about 60% of the total energy consumption of the belt conveyor [3]. So accurately predicting and reducing IRR is the focus and hot spot of current research [4–6].

The conveyor belt is mainly composed of the cover layer and core layer (i.e., skeleton material), and the core layer is bonded to the cover layer by a viscous glue. The cover layer mainly acts as a cushioning, wear-resistant layer and protects the core layer. The core material provides the strength and stiffness needed for the normal operation of the conveyor belt. The stiffness provided by the core material has a great influence on the operation resistance of the conveyor belt. Therefore, it is necessary to explain the influence of the cover rubber and the core material on the belt stiffness and IRR.

As far as performance is concerned, the rubber of the conveyor belt cover layer can be divided into soft and hard. In terms of size, the thickness is not the same. Compared with the core material, the rubber elongation of the cover layer is higher. There is a certain distance between each layer of skeleton material, that is, the so-called distance. The thickness of the different conveyor belt core layers is also different. The cover rubber and core skeleton materials have different effects

Table 1: Effect of material properties and dimension parameters of conveyor belt on bending stiffness and IRR.

Categories	Cover rubber			Core skeleton material		
Parameters	Cover thickness ↓ increase	Rubber hardness ↓ hardness	Elongation ↓ large	Core layer thickness ↓ increase	Core layer space ↓ large	Elongation ↓ small
Stiffness	Increase	Increase	Decrease	Increase	Increase	Increase
IRR	Increase	Decrease	Increase	Unknown	Unknown	Unknown

on the stiffness and IRR of the conveyor belt, as shown in Table 1.

This paper focuses on the IRR of the conveyor belt. The IRR is caused by deformation and relative movement of the viscoelastic rubber in belt contact with the rigid roller. In comparison, the influence of the core material on the IRR is very small, so it can be ignored most of the time.

The IRR is a kind of running resistance caused by deformation of material contact. Most of the earliest studies were carried out with the help of the Hertz theory model. In the paper published in 1961 by S. C. Hunter in the USA, the contact stress between a rigid cylinder (simulated roller) and a semi-infinitely long viscoelastic plane (simulated conveyor belt) was analyzed using the Hertz theory, and the formula for calculating the IRR was derived in detail [7]. In 1969, Professor F. D. S. Lynch of the USA proposed a complete numerical solution to solve the linear viscoelastic stress in a stable state by using the idea of finite element method. The boundary conditions are determined by assuming the elastic material as a linear viscoelastic material [8]. At the same time, A. Bazergui of Poland used a buried strain gauge to measure the positive stress and shear force of the contact area when the rigid cylinder was in contact with the viscoelastic material. He regarded the stress distribution in the contact area as a two-dimensional stress distribution [9].

Subsequently, on the basis of previous research results, Jonkers assumed that the cover material is a linear viscoelastic material. When the idler rolled over from the cover material, the stress variation law at a certain point in the material was analyzed. According to the corresponding relationship between IRR and energy consumption, the calculation formula of IRR was deduced [10]. The IRR formula of Jonkers gave the relationship between IRR and the load, the thickness of the cover, the diameter of the idler, the elastic modulus of the rubber of the conveyor cover, and the loss angle; the formula does not reflect the belt speed. That is the first IRR formula to reflect the viscoelastic characteristics and condition factors, and the idea of using the energy consumption method provided a useful reference for the follow-up study. In 1991, Spans used the IRR coefficient instead of the IRR to characterize the resistance [11].

In 2003, Lodewijks carried out viscoelastic tests on rubber with different compositions using a dynamic mechanical analyzer (DMA), which provided a useful reference for the study of the influence of cover layer properties on the IRR [12]. In 2006, T. J. Rudolphi and A. V. Reicks chose the generalized Maxwell model to characterize the viscoelastic properties of the cover layer and used this model to fit the results of the Lodewijks viscoelastic test. Finally, the IRR was derived with the help of the Winkler foundation [13]. However, the determination of parameters for the formula is more complicated, and the practicality is not strong. In 2012, T. J. Rudolphi and A. V. Reicks revised the calculation formula of IRR deduced in 2006. It is believed that when the load on the conveyor belt is too large, the deformation of the cover layer no longer follows the linear deformation but is a nonlinear strain [14].

In the same period, X. J. Qiu combined the energy consumption method and the main curve of the viscoelastic properties and deduced the calculation formula of IRR [15, 16]. In 2016, L. Gladysiewica proposed a new theoretical model for determining IRR and proved that the stress distribution described in the time coordinates coexists with the transverse deformation of the belt [17]. In the same year, Robinson combined the generalized Maxwell model with the spherical idler to build the model and studied the IRR of the complex idler structure and geometry [18].

Most of the above studies use mathematical reasoning to derive the calculation formula of the IRR. Some researchers use the finite element method (FEM) and boundary element method (BEM) to study the IRR. In 2006, C. Wheeler simulated the stress at points of the contact area according to the FEM [19]. In 2011, F. Qin used the FEM to analyze the stress distribution of the contact area when a moving load rolls through the rubber cover [20]. In 2012, S. Hötte focused on the deficiency of the DIIN22123 standard on the calculation method of indentation rolling resistance [21]. F. S. Wang used the BEM to deal with the rolling contact boundary conditions and verified it by example [22].

In addition to theoretical advances, test equipment for measuring the IRR is also evolving. Some studies combine theoretical research with experimental results to make the research more convincing. Professor J. I. O'Shea analyzed the errors caused by different viscoelastic testing methods on the IRR results and then introduced a dielectric model to represent the viscoelastic behavior [23, 24]. In 2016, P. Munzenberger and C. Wheeler established a test facility for testing IRR [25]. Y. Lu studied the influence law between the IRR and many factors by calculation and simplified the formula of IRR, which can directly reflect the influence of load [26–28]. J. Mao carried out experimental research on the IRR of the conveyor belt and then analyzed the dynamic characteristics of the IRR test bench of the conveyor belt [29]. H. Y. Chen calculated the IRR of the steel cord conveyor belt st3500 and compared it with the test results [30].

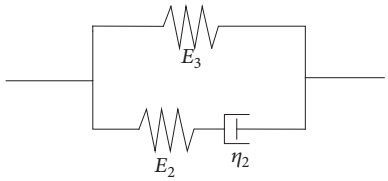

Figure 1: The three-element Maxwell solid model.

The circumstance temperature has an important effect on the properties of the polymer material in the belt cover. However most of the above studies did not take into account the effects of temperature, or the ambient temperature was presented, but the relationship between the temperature and the IRR was not reflected visually.

Moreover, all the above test systems for IRR cannot control the ambient temperature, which is a little insufficient. Therefore, this paper focuses on deducing the mathematical model of IRR with temperature parameters and establishes a measurement system with a temperature control chamber.

Based on the three-element Maxwell solid model and under different temperatures, the dynamic loading experiments of cylindrical rubber made of conveyor belt cover material were performed to receive the identification models of elastic moduli E_2 and E_3 and viscosity coefficient η_2. And then the fitting functions of these three parameters are obtained. After that, the mathematical model of the IRR considering the ambient temperature is deduced. The effect of temperature on rolling resistance of collapse is reflected by the elastic modulus and viscous coefficient. And the influence law of various factors on rolling resistance of collapse is studied according to the working conditions of different ambient temperatures, belt speeds, vertical loads, idler radii, and thicknesses of underlying rubber. Finally, experimental verification is accomplished.

2. Experimentally Obtaining the Viscoelastic Parameters Functions of the Conveyor Belt

2.1. Theoretical Basis. The three-component Maxwell solid model can well characterize the viscoelastic properties of rubber materials, so it is chosen as the constitutive model to study the changes of rubber constitutive parameters at different temperatures. The model is shown in Figure 1.

The stress relaxation function of the three-element Maxwell solid model is

$$\psi(t) = E_3 + E_2 e^{-t/\tau}, \tag{1}$$

where E_2 and E_3 are the moduli, t is the time, and τ is the lag time, $\tau = \eta_2/E_2$.

The constitutive relation of the model is expressed as follows:

$$\sigma + p_2\dot{\sigma} = q_2\varepsilon + q_3\dot{\varepsilon}, \tag{2}$$

where σ and ε are the stress and strain, respectively. p_2, q_2, and q_3 are the model parameters, respectively.

$$\begin{aligned} p_2 &= \frac{\eta_2}{E_2}, \\ q_2 &= E_3, \\ q_3 &= \frac{E_2 + E_3}{E_2}\eta_2. \end{aligned} \tag{3}$$

The above formulas are common and are the basis of research. The following is the derivation of the formula for the specific situation of this paper.

If the sinusoidal displacement excitation is applied to the conveyor belt with length H, the expression of the excitation is as follows:

$$B = A_0 + A\sin(\omega t), \tag{4}$$

where A_0 is the initial displacement, A is the amplitude, and ω is the angular frequency.

According to the displacement response (4), the corresponding strain function can be obtained, which is

$$\varepsilon = \frac{A_0}{L} + \frac{A}{L}\sin(\omega t). \tag{5}$$

The expression formula of strain function (5) is substituted into constitutive equation (2), and the result is

$$\sigma + p_2\dot{\sigma} = q_2\left(\frac{A_0}{L} + \frac{A}{L}\sin\omega t\right) + q_3 \cdot \frac{A\omega}{L}\cos\omega t. \tag{6}$$

The steady-state solution of stress is obtained by solving (6), which is as follows:

$$\begin{aligned} \sigma = q_0\frac{A_0}{H} &+ \frac{A\omega(q_3 - q_2p_2)}{H(1+\omega^2p_2^2)}\cos(\omega t) \\ &+ \frac{A(q_3\omega^2p_2 + q_2)}{H(1+\omega^2p_2^2)}\sin(\omega t). \end{aligned} \tag{7}$$

Then the dynamic force of the conveyor belt under displacement excitation can be expressed as

$$\begin{aligned} F = q_2\frac{A_0}{H}S &+ \frac{A(q_3 - q_2p_2)\omega S}{H(1+\omega^2p_2^2)}\cos(\omega t) \\ &+ \frac{AS(p_2q_3\omega^2 + q_2)}{H(1+\omega^2P_2^2)}\sin(\omega t), \end{aligned} \tag{8}$$

where F is the force under strain and S is the cross-sectional area of the belt.

Order $c_0 = q_2(A_0/H)S$, $c_1 = (A(q_3 - q_2p_2)\omega/H(1 + \omega^2p_2^2))S$, and $c_2 = (A(p_2q_3\omega^2 + q_2)/H(1 + \omega^2P_2^2))S$.

Then (8) is transformed into

$$F = c_0 + c_1 * \cos(\omega t) + c_2\sin(\omega t). \tag{9}$$

Formula (9) is the same as the first-order Fourier series.

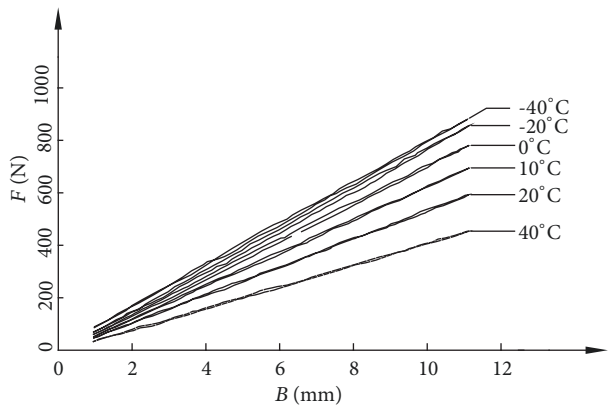

Figure 2: Experimental curve at different temperatures.

2.2. Obtaining of Viscoelastic Parameter Function. The performance categories of conveyor belt cover are specified in GB/T 33525-2017, including category H for severe cut and gouge service and category D for severe abrasion service and moderate service. The rubber material used in the test here is category L cover rubber. The conveyor belt with L-type cover rubber can transport moderately worn materials or slightly worn or nonworn dry materials. It is the most common type of conveyor belt cover in China. The rubber was molded into a rubber cylindrical sample with a radius of 50 mm and a height of 100 mm [30].

The dynamic tensile test of the cylinder cover rubber was completed to determine the elastic modulus of the cover layer and the viscosity coefficient as a function of temperature. In order to quantitatively analyze the effect of temperature on the material properties of the conveyor belt, the viscoelastic three-element Maxwell solid model is used as the constitutive model.

Before starting the dynamic tensile displacement experiment, the temperature of the temperature control box is adjusted to -20, -10, 0, 10, 20, and 40°C, respectively, and kept for three hours to ensure that the rubber sample reaches their respective temperature characteristics, and then the dynamic tensile test was carried out. The dynamic compression tests were fulfilled on a high and low temperature universal testing machine. Test temperature is adjusted by the temperature control box.

At six different temperatures, a sinusoidal displacement excitation of (4) is applied to the conveyor belt, with an initial compression displacement $A_0 = 6$ mm and an amplitude $A = 5$ mm. According to the test results, the graph shown in Figure 2 can be obtained.

As can be seen from Figure 2, the dynamic force-displacement curve of rubber decreases obviously with the increase of temperature. At the same time, the area of the hysteresis loop surrounded by the force-displacement curve decreases gradually. It can clearly be seen that the influence of temperature on the parameters of the rubber constitutive model is obvious.

Figure 2 is the same as that expressed by (9), which is the theoretical foundation of the test. Therefore, the curve of Figure 2 is fitted by formula (9); that is, the first-order Fourier series is used to fit and analyze the external load F. The coefficients corresponding to formula (9) at different temperatures are obtained from six curves in Figure 2. The values are listed in Table 2.

Table 2: c_0, c_1, and c_2 at different temperatures.

T [°C]	-20	-10	0	10	20	40
c_0	470.17	467.47	422.00	355.23	288.81	243.67
c_1	161.46	152.89	121.41	84.76	55.65	39.56
c_2	391.89	389.72	351.72	296.05	240.68	203.07

According to the expressions c_0, c_1, and c_1, the expressions of model parameters p_2, q_2, and q_3 can be obtained, which are as follows:

$$p_2 = \frac{A_0 c_2 - A c_0}{A_0 c_1 \omega} \tag{10}$$

$$q_2 = c_0 \frac{H}{A_0 S} \tag{11}$$

$$q_3 = \frac{q_2 (c_1 + p_2 c_2 \omega)}{c_2 \omega - c_1 \omega^2 p_2}. \tag{12}$$

Combining formulas (3), (10), (11), and (12), the identification model of the three-element Maxwell solid model parameters can be obtained as follows:

$$E_2 = \frac{H \left(A_0^2 c_1^2 + A_0^2 c_2^2 - 2AA_0 c_1 c_2 + A^2 c_0^2\right)}{AA_0 S \left(c_2 A_0 - A c_0\right)} \tag{13}$$

$$E_3 = \frac{c_0 H}{A_0 S} \tag{14}$$

$$\eta_2 = \frac{H \left(A_0^2 c_1^2 + A_0^2 c_2^2 - 2AA_0 c_1 c_2 + A^2 c_0^2\right)}{AA_0^2 c_1 \omega S}. \tag{15}$$

The values of the parameters in (13), (14), and (15) are known or calculated so that elastic modulus values E_2 and E_3 and viscous coefficient value η_2 can be acquired at different temperatures. Then the parameters are fitted by MATLAB. In order to better observe the changing trend of elastic modulus and viscous coefficient, the polynomial is used to fit the elastic modulus and viscous coefficient. The results are as follows:

$$E_2 = -3.593 \times 10^5 T^3 + 1.449 \times 10^7 T^2 + 5.167 \times 10^8 T + 9.407 \times 10^9 \tag{16}$$

$$E_3 = 7.653T^3 - 225.6T^2 - 1.268 \times 10^4 T + 8.956 \times 10^5 \tag{17}$$

$$\eta_2 = -0.1296T^3 - 0.04417T^2 + 510.3T + 8.907 \times 10^4. \tag{18}$$

The R-square values of the three curves of the elastic modulus and viscosity coefficient are 0.9833, 0.998, and 0.998, respectively. It can be seen that the three curves have high fitting accuracy.

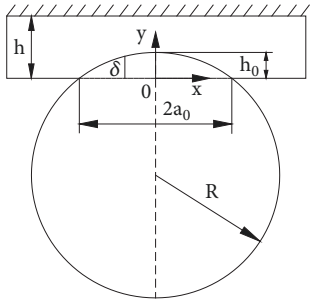

Figure 3: Geometric model of static indentation zone.

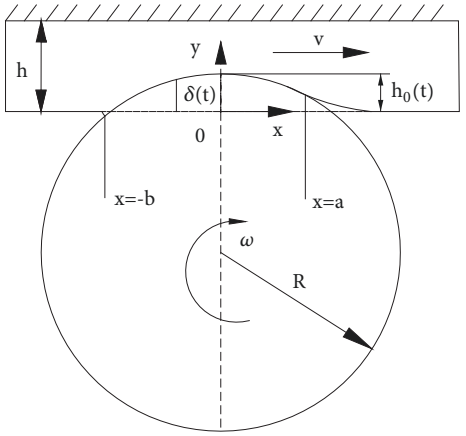

Figure 4: Geometry model of dynamic indentation zone.

3. Mathematical Model of IRR

3.1. Static Indentation Analysis. The indentation state between the cover layer under the conveyor belt and the intermediate flat idler under static state is studied. The geometric model is shown in Figure 3 [27]. The geometric model is based on several hypotheses, which are as follows: (1) On the full thickness, the cover layer of the conveyor belt is isotropic. (2) The thickness of cover layer h is greater than the depression deformation. (3) The contact half-length is less than the roller radius R.

The compression deformation of conveyor belt δ is as follows:

$$\delta = \sqrt{R^2 - x^2} - R + h_0 \approx h_0 - \frac{x^2}{2R}, \tag{19}$$

where δ is the deformation of belt, R is the radius of idler, and h_0 is the maximum indentation depth of the belt in static state.

The strain in the contact area between the conveyor belt and idler is

$$\varepsilon = \frac{\delta}{h} = \frac{h_0}{h} \sin\left(\frac{\pi}{2} - \beta\right), \tag{20}$$

where ε is the strain in the contact area between belt and idler, h is the thickness of cover layer, and $\beta = (\sqrt{2}/a_0)x(-a_0 < x < a_0)$.

The stress σ_0 corresponding to (16) is

$$\sigma_0 = \frac{h_0\left(E_2 + E_3\right)}{h} \cos\beta. \tag{21}$$

From the vertical balance condition, the positive pressure of the unit width between the idler and belt is received as follows:

$$P = \int_{-a_0}^{a_0} \sigma_0 dx = \sqrt{2} \times \sin\sqrt{2} \times \frac{h_0}{h} a_0\left(E_2 + E_3\right). \tag{22}$$

According to the geometric relationship $a_0^2 + (R - h_0)^2 = R^2$ in Figure 3, $h_0 \approx a_0^2/2R$ is available. Because $\sin\sqrt{2} \approx 1$, the positive pressure is transformed into

$$P = \frac{a_0^3}{\sqrt{2}Rh}\left(E_2 + E_3\right). \tag{23}$$

The mathematical model of the half-length a_0 of the contact area can be gotten:

$$a_0 = \left(\frac{\sqrt{2}PRh}{E_2 + E_3}\right)^{1/3}. \tag{24}$$

The analysis of the static indentation state of the belt is the basis for the dynamic IRR. For this section, the derived mathematical model of a_0 is the key, which plays an important role in calculating IRR.

3.2. Establishment of Mathematical Model of Dynamic IRR. When the belt conveyor is in operation, the geometric model of the indentation rolling resistance is shown in Figure 4, which assumes that the belt conveyor is operating at a constant speed [26].

As can be seen from Figure 4, the contact arc of the conveyor belt and the idler roller is no longer symmetrical with respect to the center line of the idler roller, which is due to the viscoelastic properties of the underlying cover layer.

At this point, the dynamic strain of conveyor belt is

$$\varepsilon(t) = \frac{\delta(t)}{h} = \frac{v}{2Rh}\left(2at - vt^2\right), \tag{25}$$

where $\varepsilon(t)$ is the dynamic strain, $\delta(t)$ is the dynamic deformation of belt, v is belt speed, and a is the length of the contact area at $x = a$.

The relaxation constitutive equation of viscoelastic materials is

$$\sigma(t) = \varepsilon_0\psi(t) + \int_0^t \psi(t - \tau)\, d\varepsilon(\tau). \tag{26}$$

The available stress expression is

$$\sigma(t) = \frac{E_3}{2Rh}\left(2at - t^2v^2\right) + \frac{a^2kE_2}{Rh}\left((1 + k)\left(1 - e^{-tv/ka} - \frac{tv}{a}\right)\right). \tag{27}$$

The absolute coordinate of the point $x = a$ at any time is $x = a - vt$; then the indentation stress of any point in the indentation area is

$$\sigma(x) = \frac{E_3\left(a^2 - x^2\right)}{2Rh} + \frac{a^2kE_2}{Rh}\left((1+k)\left(1 - e^{(x-a)/ak}\right) - \frac{a-x}{a}\right). \tag{28}$$

The force analysis of the conveyor belt in the indentation zone is completed under the condition that the belt speed remains unchanged. According to the equilibrium conditions in the vertical direction, the expression of the vertical load can be gotten as follows:

$$P = \frac{a^3E_3}{6Rh}\left(-\lambda^3 + 3\lambda + 2\right) + \frac{a^3kE_2}{Rh}(1+k)\left(1 + \lambda - k + ke^{-(1+\lambda)/k}\right) - \frac{a^3kE_2}{2Rh}\cdot(1+\lambda)^2, \tag{29}$$

where $\lambda = b/a$ and $k = v\tau/a$.

The resistance moment of the stress distribution on the conveyor belt to the center of the idler is as follows:

$$M = \int_{-b}^{a} x\sigma(x)\,dx. \tag{30}$$

Combining (28) and (29), the mathematical model of the IRR is

$$F_z = \frac{a^4E_3}{8R^2h}\left(\lambda^4 - 2\lambda^2 + 1\right) + \frac{a^4kE_2}{R^2h}\left[\frac{1+\lambda^3}{3} - \frac{k}{2}\cdot\left(1+\lambda^2\right) + k^3\right] - \frac{a^4kE_2}{R^2h}k(k+\lambda)(1+k)e^{-(1+\lambda)/k}. \tag{31}$$

By the perfect combination of formulas (16), (17), and (18) and formula (31), a new mathematical model for IRR is obtained, which is as follows:

$$\begin{aligned} F_z = {} & \frac{a^4}{8R^2h}\left(\lambda^4 - 2\lambda^2 + 1\right)\left(7.653T^3 - 225.6T^2\right. \\ & \left. - 1.268\times10^4T + 8.956\times10^5\right) + \frac{a^4k}{R^2h}\left(-3.593\right. \\ & \left.\times10^5T^3 + 1.449\times10^7T^2 + 5.167\times10^8T + 9.407\right. \\ & \left.\times10^9\right)\left[\frac{1+\lambda^3}{3} - \frac{k}{2}\cdot\left(1+\lambda^2\right) + k^3\right] \\ & - \frac{a^4k}{R^2h}\left(-3.593\times10^5T^3 + 1.449\times10^7T^2 + 5.167\right. \\ & \left.\times10^8T + 9.407\times10^9\right)k(k+\lambda)(1+k)e^{-(1+\lambda)/k}. \end{aligned} \tag{32}$$

The mathematical model not only includes parameters such as belt speed, idler radius, and cover thickness, but also directly reflects the influence of temperature on IRR. This is a new mathematical model, which has never appeared before. The relationship between the IRR and the vertical load is indirectly reflected by a and b. The viscosity coefficient η_2 is indirectly reflected by the parameter k.

4. Analysis of Theoretical Results

The IRR is directly related to the parameters such as the belt speed v, the viscoelastic characteristics E_2, E_3, and η_2, the idler radius R, and the thickness h of the cover layer and is indirectly related to the ambient temperature T and the normal force P. In this section, the influence of various factors on IRR is studied in detail.

According to the temperature change throughout the year, -20°C ~ 40°C are chosen as the ambient temperature of the belt conveyor. Generally, the belt speed ranges from 0.1 m/s to 6.5 m/s, but, for long-distance and large-capacity belt conveyors, the belt speed takes a larger value, so this paper chooses the belt speeds of 1, 2, 3, 4, 5, 6, 7, 8, 9, and 10 m/s.

The normal force P applied to the belt is in the range of $n \times 600$ N/m, $n = 1, 2, \ldots, 5$. The roller radius R takes the values of 38, 44.5, 54, 66.5, and 79.5, and the unit is mm. The common values of 1.5, 3.0, 5, 6, 8, and 10 are selected as the thickness h of the cover layer and the unit is mm. All the above values are selected according to the actual engineering conditions. At the same time, the theoretical analysis in this section is fulfilled for the above different conditions.

Firstly, the simulation experiment research of the influence of belt speed on the IRR is carried out. In the test, the working temperature of the conveyor belt is -20°C, and the radius of the idler is 0.0445 m. These two factors remain unchanged and 6 groups of numerical simulations are carried out. In the first set of simulations, the thickness of the cover layer is 0.0015 m, and the vertical load is 600 N/m–3000 N/m. The IRR at different belt speeds is analyzed. The difference of each group is the change of the thickness of the cover layer, which is 0.0015 m, 0.003 m, 0.005 m, 0.006 m, 0.008 m, and 0.01 m, respectively. That is to say, the influence of velocity on the IRR is analyzed when the thickness of the cover layer is different. The numerical simulation results are shown in Figures 5–10.

It can be seen from Figures 5–10 that the influence of velocity on the IRR is complicated, and it is not a simple linear relationship. The overall trend of the curves shows that as the belt speed increases gradually, the indentation rolling resistance gradually decreases. When the belt speed is less than 6 m/s, the IRR decreases greatly. Therefore, in this range, enterprises can increase the speed of belt conveyor appropriately according to the actual working conditions to achieve the purpose of energy saving. When the belt speed is greater than 6 m/s, the reduction of IRR is less.

Specifically, the curve in Figure 7 with a vertical load of 3000 N/m is analyzed. When the speed is 1 m/s, the IRR is 177.3 N/m, which is the maximum value in the figure. When the speed is increased by 10 m/s, the IRR is 51.2 N/m. The IRR

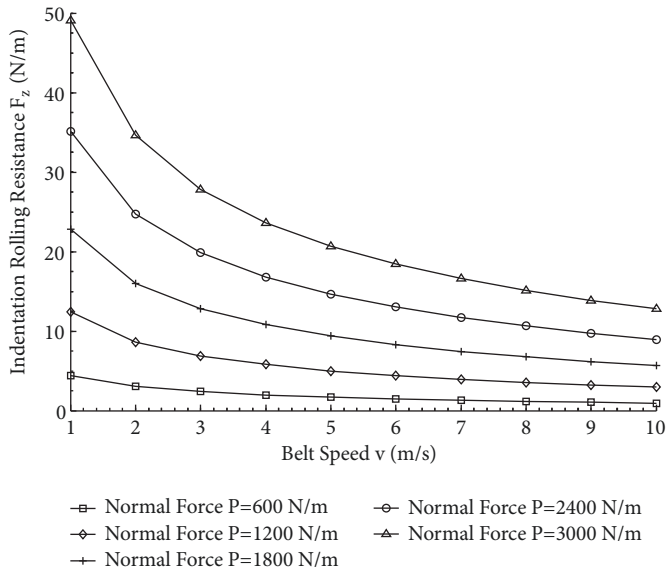

Figure 5: Relationship diagram between belt speed and IRR—T=-20°C, R=0.0445 m, h=0.0015 m.

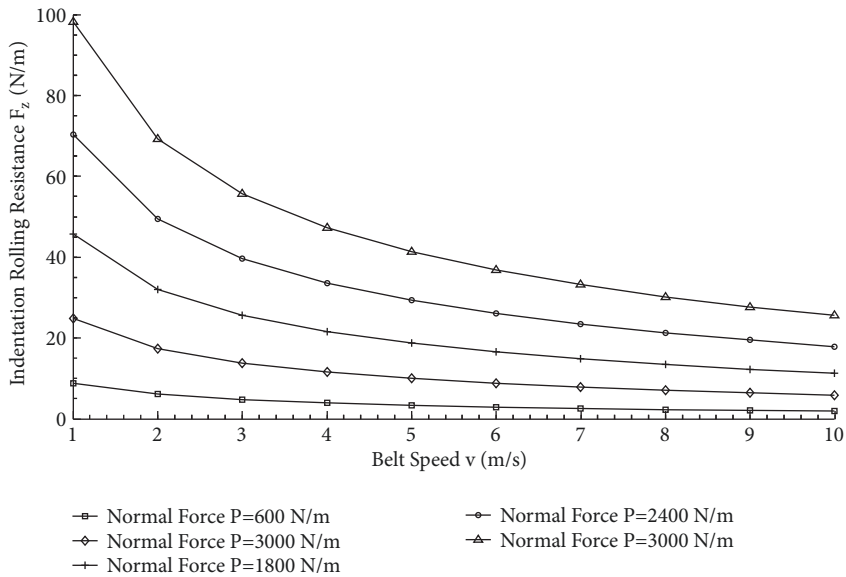

Figure 6: Relationship diagram between belt speed and IRR—T=-20°C, R=0.0445 m, h=0.003 m.

is reduced by 71.12%. It can be seen that the influence of the belt speed on the IRR is large.

Figures 5–10 also fully illustrate the influence of the thickness of the cover layer. It is also found that the increase of the thickness of the cover layer does not affect the trend of the influence of the belt speed on the indentation rolling resistance. The IRR increases greatly with the increase of the thickness of the cover layer, especially when it is increased from a 1.5 mm to 5 mm process. In Figure 5, the thickness of the cover layer is 0.0015 m, the vertical load is 2400 N/m, and the belt rolling speed is 1 m/s, and the IRR is 70.3 N/m. In Figure 5, the remaining parameters are the same and the thickness of the cover layer is increased to 0.01 m. In the case, the IRR is 178.1 N/m, and IRR is increased by 60.53%.

In the study of ambient temperature and IRR, the range of temperature varies within -20°C~40°C. The research on temperature is divided into two parts. In the first part, the belt speed, roller radius, and cover thickness are fixed parameters. The effect of temperature change on IRR under different forces is analyzed. The simulation results are shown in Figures 11 and 12. In the second part, the normal force, roller radius, and cover thickness are fixed parameters. The effect of temperature change on IRR under different belt speeds is analyzed. The results are shown in Figure 13.

Figures 11–13 show when the vertical load is small (less than or equal to 1800 N/m), and the increase of temperature causes the fluctuation of IRR at a very small range. The IRR shows a trend of being flat or even slightly increased and

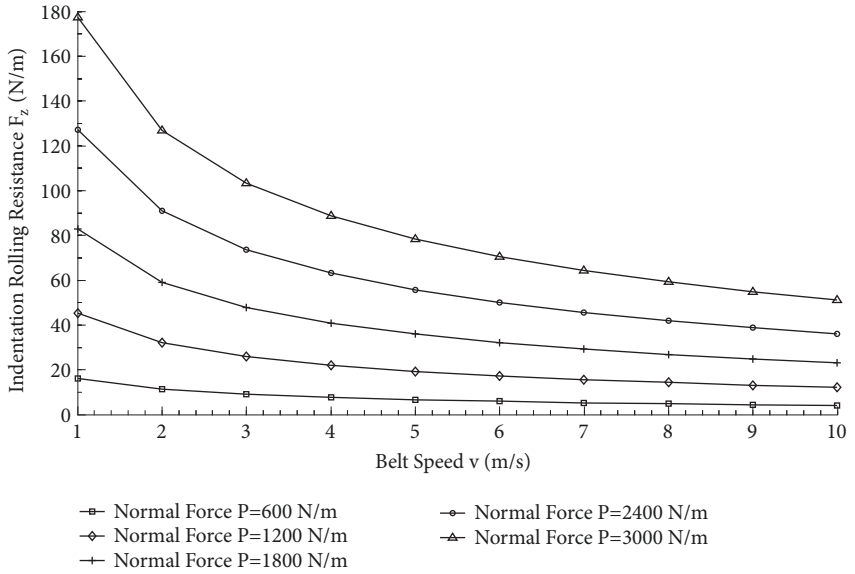

Figure 7: Relationship diagram between belt speed and IRR—T=-20°C, R=0.0445 m, h=0.005 m.

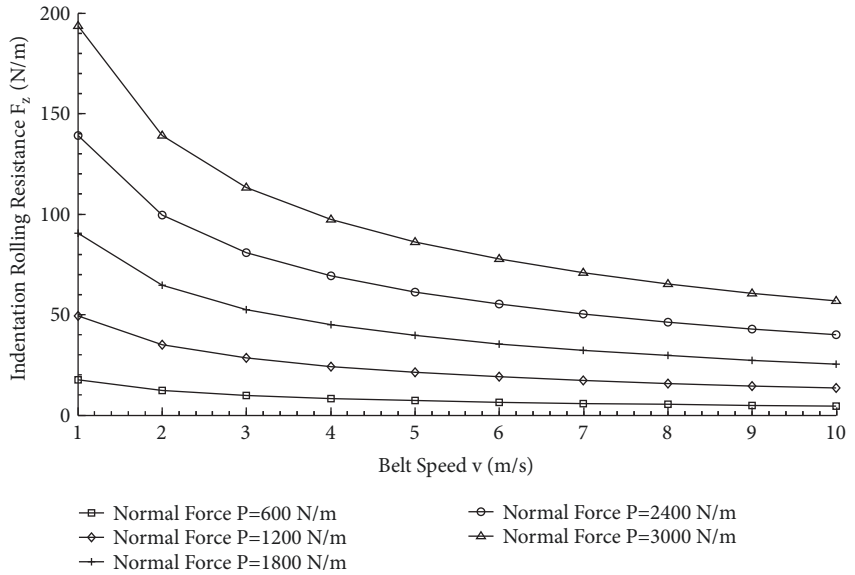

Figure 8: Relationship diagram between belt speed and IRR—T=-20°C, R=0.0445 m, h=0.006 m.

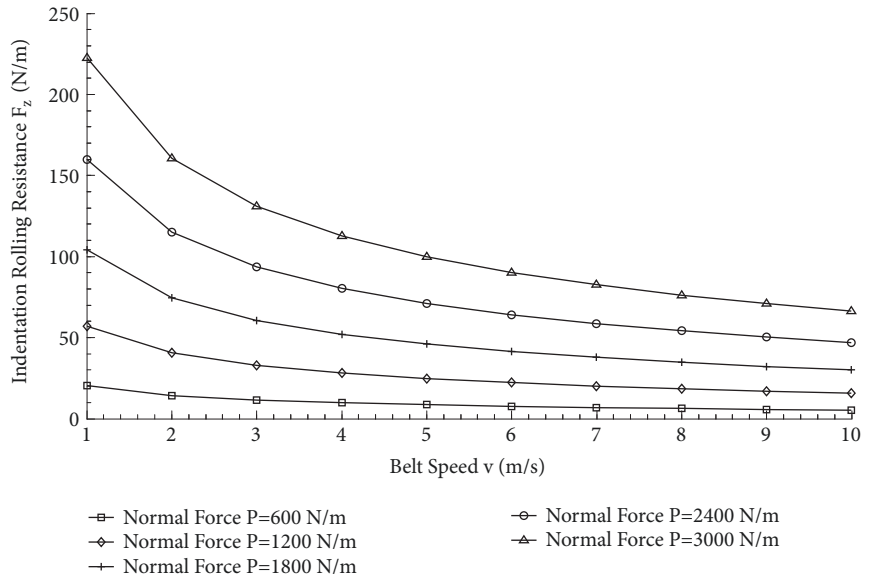

Figure 9: Relationship diagram between belt speed and IRR—T=-20°C, R=0.0445 m, h=0.008 m.

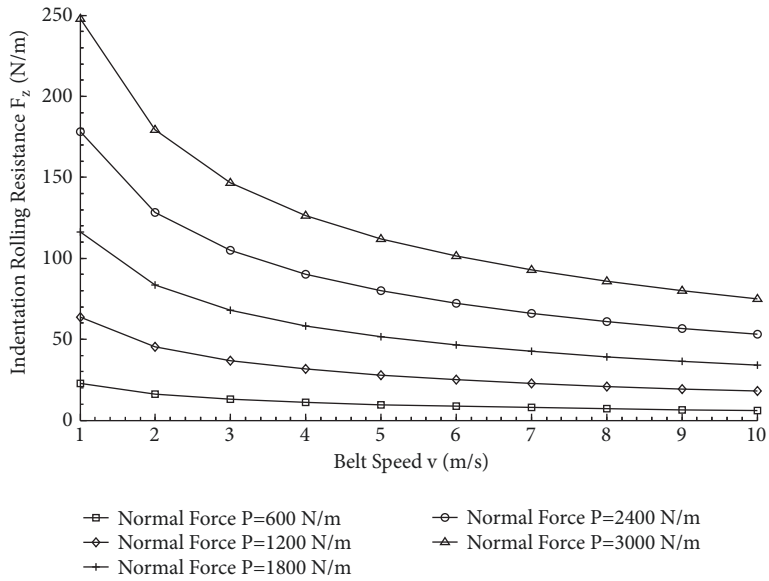

Figure 10: Relationship diagram between belt speed and IRR—T=-20°C, R=0.0445 m, h=0.01 m.

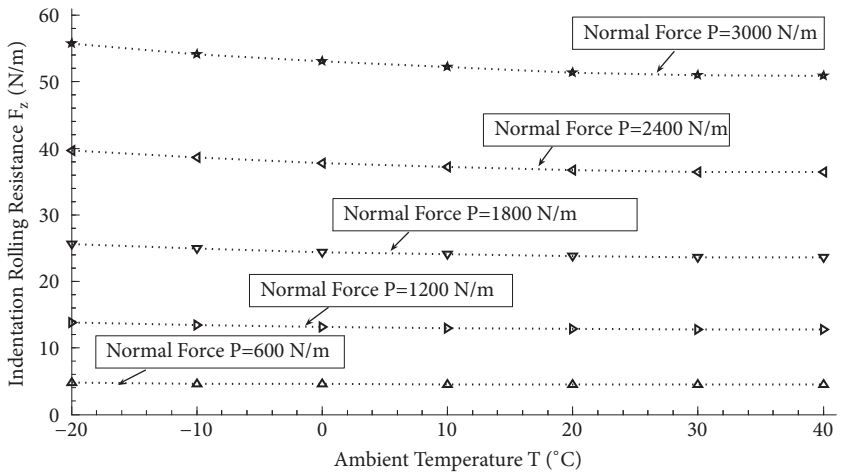

Figure 11: Relationship diagram between ambient temperature and IRR—v=3 m/s, R=0.0445 m, h=0.0015 m.

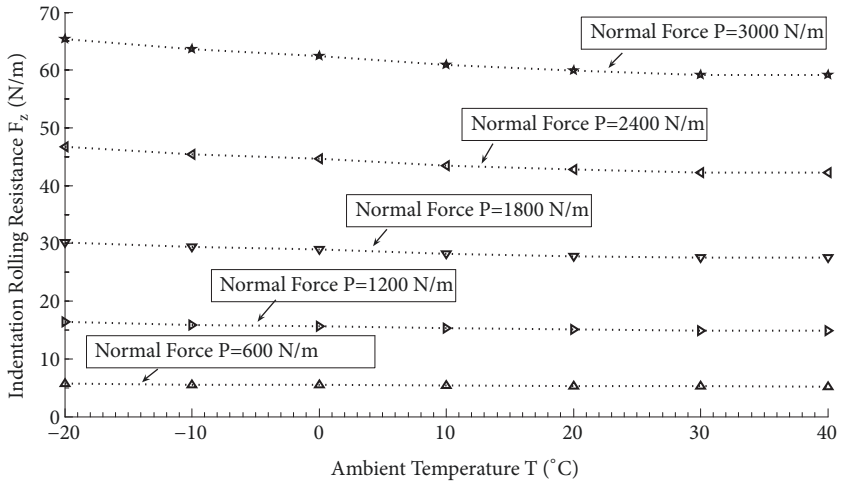

Figure 12: Relationship diagram between ambient temperature and IRR—v=3 m/s, R=0.0665 m, h=0.003 m.

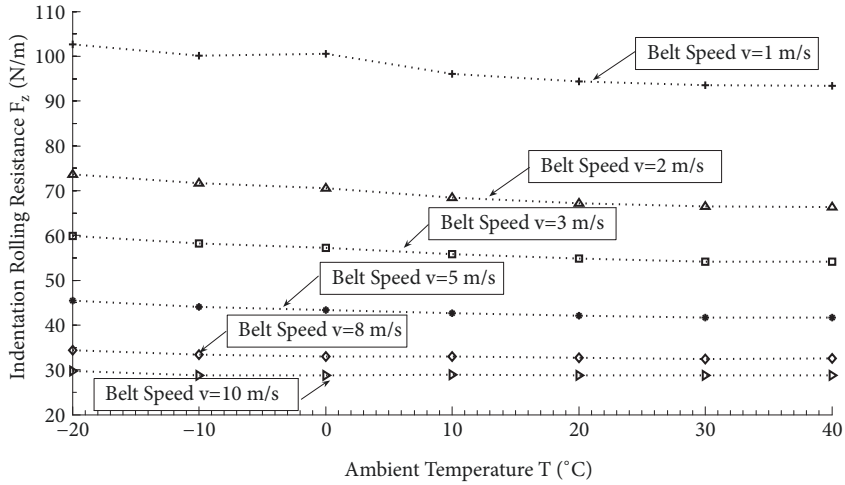

Figure 13: Relationship diagram between ambient temperature and IRR—P=3000 N/m, R=0.0795, h=0.003 m.

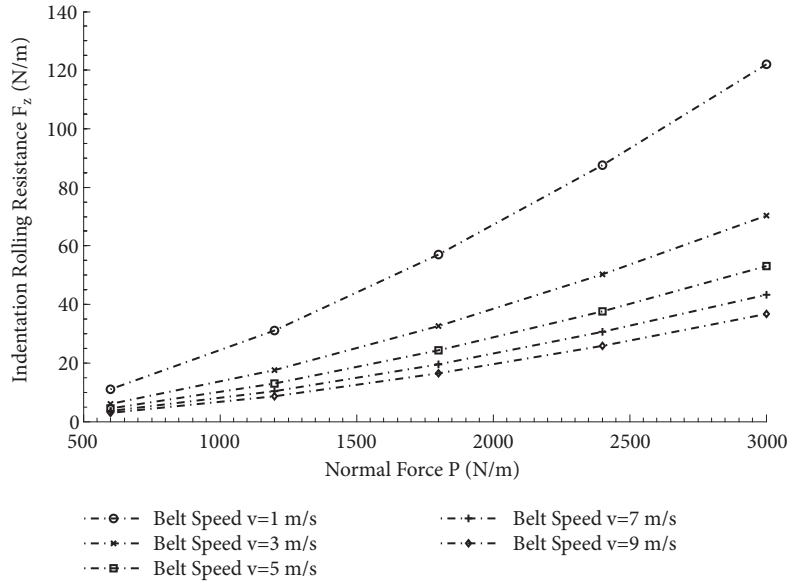

Figure 14: Relationship diagram between normal force and IRR—T=-10°C, R=0.054 m, h=0.003 m.

then decreased, of course, in a small range of changes. When the vertical load is greater than 1800 N/m, an increase in temperature results in a gradual decrease in the indentation rolling resistance. Under the combined action of belt velocity and temperature, the curve of IRR is complex. At the speed of 1 m/s, IRR increases locally and then decreases. After the speed is greater than 1 m/s, the IRR is gradually reduced in steps of less than 1 N/m.

The maximum IRR is 73.6 N/m when the belt speed is 2 m/s in Figure 13. With the increase of temperature, the IRR gradually decreases, and the temperature reaches 40°C and reaches the minimum value of 66.4 N/m. The IRR is decreased by 9.78%. The effect of temperature on the IRR is small, but it cannot be ignored.

Then the normal force and the IRR are studied, which are divided into three groups to carry out simulation experiments. The ambient temperature in each of the three groups is -10°C, and the belt speed is 1 m/s, 3 m/s, 5 m/s, 7 m/s, and 9 m/s. In the first group and the second group of simulation tests, the thickness of the cover layer is the same and the radii of the idler are different. The relationship between normal force and IRR is studied. The results are shown in Figures 14 and 15. The third group of simulation tests is to compare with the second group. The difference between them are the values of the thickness of the cover layer and the results are shown in Figure 16.

Observing Figures 5–7 and Figures 14–16, it can be found that, with the increase of vertical load, the IRR increases gradually, and the increasing rate of IRR is related to belt speed. When the belt speed becomes lower and the normal force greater, the IRR is maximum, and vice versa.

In Figure 14, on the curve with a belt speed of 1 m/s, the maximum IRR is obtained under the corresponding load. When the normal force is 600 N/m, the IRR is 11 N/m and

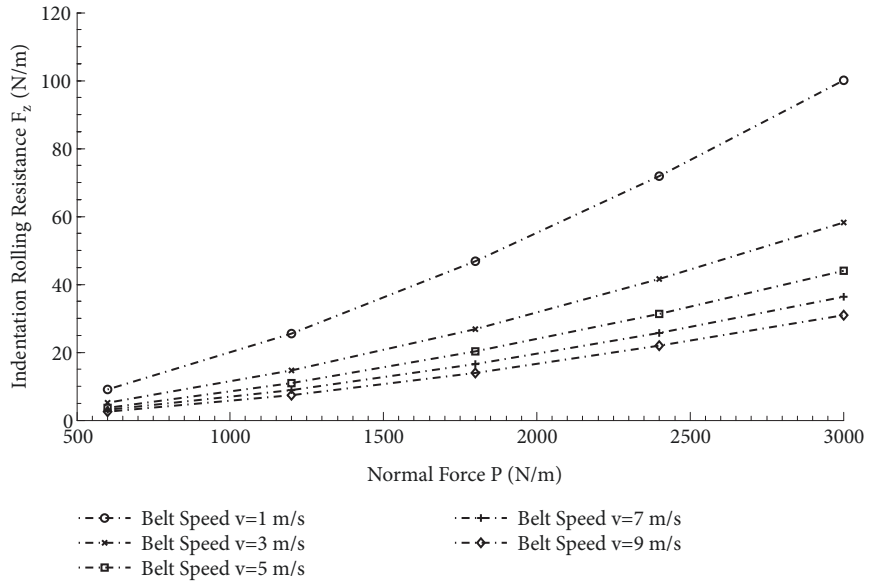

Figure 15: Relationship diagram between normal force and IRR—T=-10°C, R=0.0795 m, h=0.003 m.

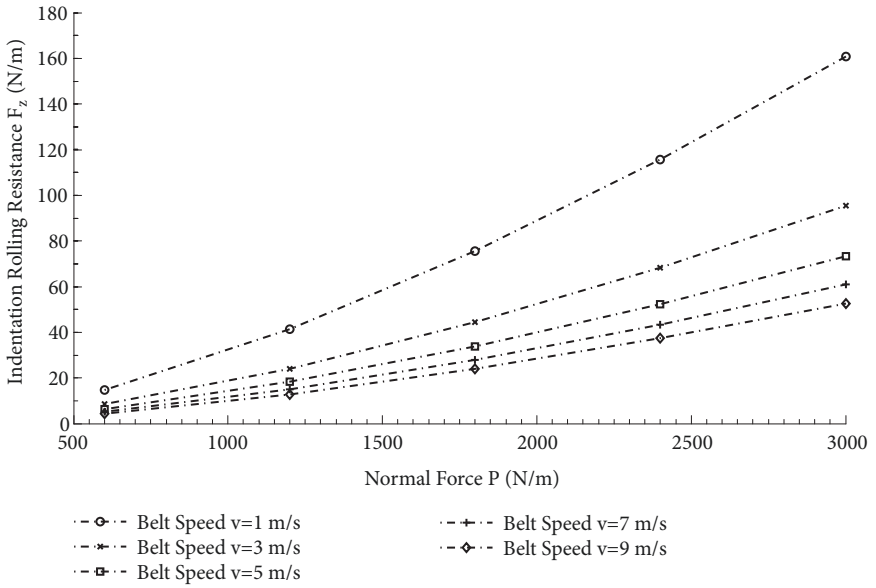

Figure 16: Relationship diagram between normal force and IRR—T=-10°C, R=0.0795 m, h=0.008 m.

when the normal force is increased to 3000 N/m, the IRR is 122 N/m. The IRR is increased by 90.98%. Therefore, it is not easy for the large-capacity belt conveyor to obtain a small IRR.

The effect of idler radius is analyzed under the comprehensive working conditions of 20°C, 1800 N/m of normal force, and 0.003 m thickness of cover layer. The results are shown in Figure 17. From Figures 14, 15, and 17, it can be seen that the increase of the idler radius is accompanied by the reduction of IRR, and the effect is obvious. When the velocity is 1 m/s in Figure 14, the IRR is the largest which is 122 N/m. In Figure 15, the maximum indentation resistance is 100.1 N/m at a speed of 1 m/s. Therefore, at a temperature of -10°C, the idler radius is increased from 0.054 m to 0.0795 m, and the IRR is reduced by 17.95%. On the curve of 2 m/s belt speed in Figure 17, when the radius of idler is 0.038 m, the IRR is 45.1 N/m. When the radius of idler is increased to 0.0795 m, the IRR is 31.2 N/m, which reduces by 30.82%.

5. Experiment and Verification

In order to verify the validity of the theory of IRR in this paper, we design and build IRR test equipment, as shown in Figure 18. The experimental tests can be carried out with any combination of different idler radii R, different vertical loads P, and different belt speeds v at different temperatures for different conveyor belts.

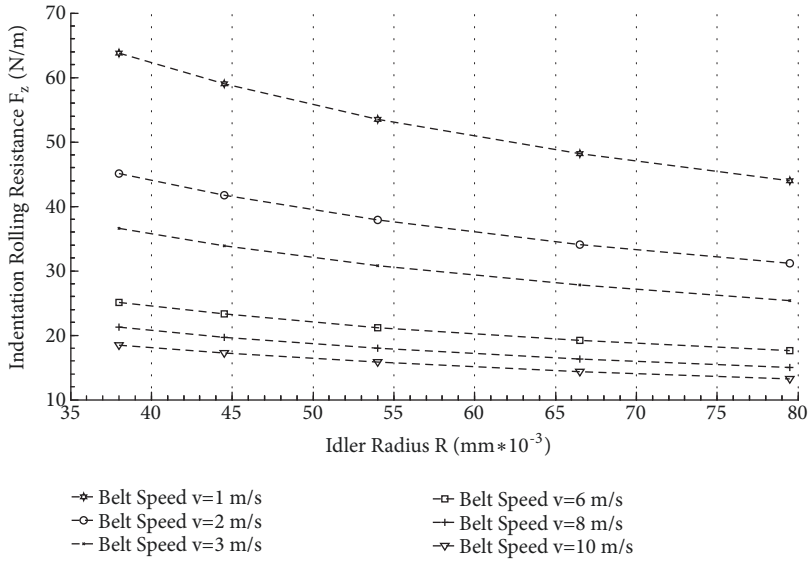

Figure 17: Relationship diagram between idler radius and IRR—T=20°C, P=1800 N/m, h=0.003 m.

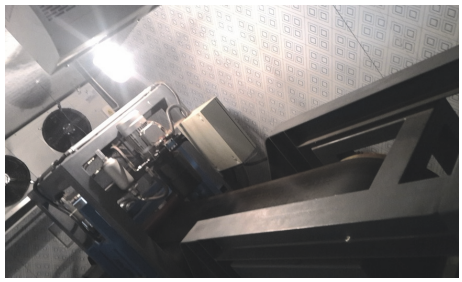

Figure 18: Indentation rolling resistance test system.

Figure 20: Display and control panel.

Figure 19: Temperature control room.

The temperature of the environmental control chamber (shown in Figure 19) is adjusted to the desired temperature by operating on the temperature control panel. It should be noted that the entire experimental system needs to be stationary for 3 hours at a certain experimental temperature before each loading, so that the characteristics of the entire indentation rolling resistance test system are consistent.

In the test, belt speed and normal force can be changed by corresponding operations in the control panel (shown in Figure 20). A fabric conveyor belt with 400 mm width and 6 mm thickness of backing cover was selected in the experiment. The experimental idler diameter is 89 mm. Under different working conditions, each experiment is accomplished three times, and the average value is finally obtained. The experimental results are shown in Figures 21–23.

Figure 21 is a comparison of experimental results and theoretical calculations of the indentation rolling resistance under different ambient temperatures. The normal forces applied in the experiment are 600 N/m and 1800 N/m, respectively. Figure 22 is a comparison of experimental and theoretical results of the indentation rolling resistance at the temperatures of 0°C and 30°C for different belt speeds. Figure 23 is a comparison between the experimental and theoretical results under different normal forces with belt speeds of 3 m/s and 4 m/s. It can be seen that the trend of experimental results is basically consistent with that of theoretical results. However, most of the experimental values of IRR are larger than the theoretical ones, which may be due to the influence of roller resistance and sensor resistance during the actual operation of belt conveyor. In order to achieve the purpose of energy saving of belt conveyor in actual working conditions, it is necessary to take into account the influence of various factors.

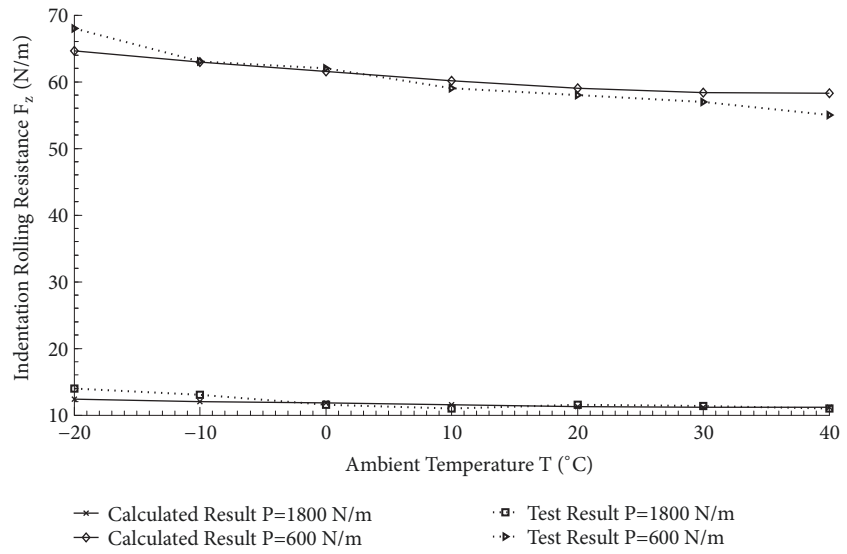

Figure 21: Comparison diagram of theoretical results and experimental results at different temperatures—v=2 m/s, R=0.0445 m, h=0.006 m.

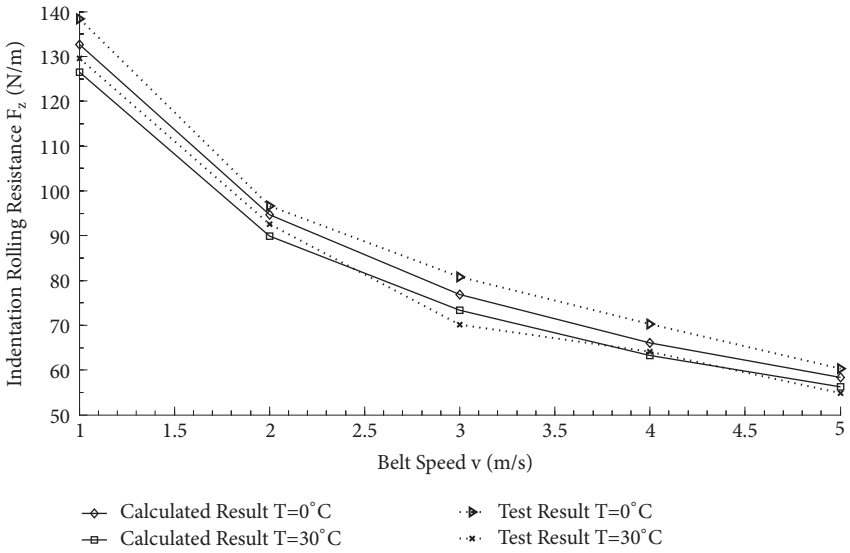

Figure 22: Comparison diagram of theoretical results and experimental results at different speeds—P=2400 N/m, R=0.0445 m, h=0.006 m.

6. Application Analysis

The theoretical and experimental results obtained in this paper can be used to calculate and judge the IRR of a conveyor belt in practical engineering and then provide guidance on how to reduce the energy consumption of the belt conveyor.

(1) Matching Selection of Conveyor Belt and Working Condition Environment. Belt conveyors are widely used in ports, mines, extremely cold areas, and other different occasions. For example, when the northern part of China is in the winter, while some parts of southern China are summer, it can be seen that the temperature varies greatly from place to place. According to different working conditions, it is wise to choose the conveyor belt with low energy consumption. Paper [24] compares the power changes of two different conveyor belts at -10°C and 40°C, as shown in Figure 24. The information we can get from the graph is that it is more appropriate to select conveyor belt B under the hot working conditions, such as 40°C, and the choice of conveyor belt A is more suitable in the colder places, such as -10°C.

The environmental conditions of conveyor belts are complex, not only the difference of temperature. According to the research in this paper, the IRR of different conveyor belts in their respective environments can be obtained, and then the power can be calculated. By comparing and analyzing, the belt conveyor which is more suitable for working conditions can be selected.

(2) Development of Low IRR of Conveyor Belt. For a belt conveyor, about 60% of energy consumption is used to overcome the IRR of conveyor belt through the idler rollers.

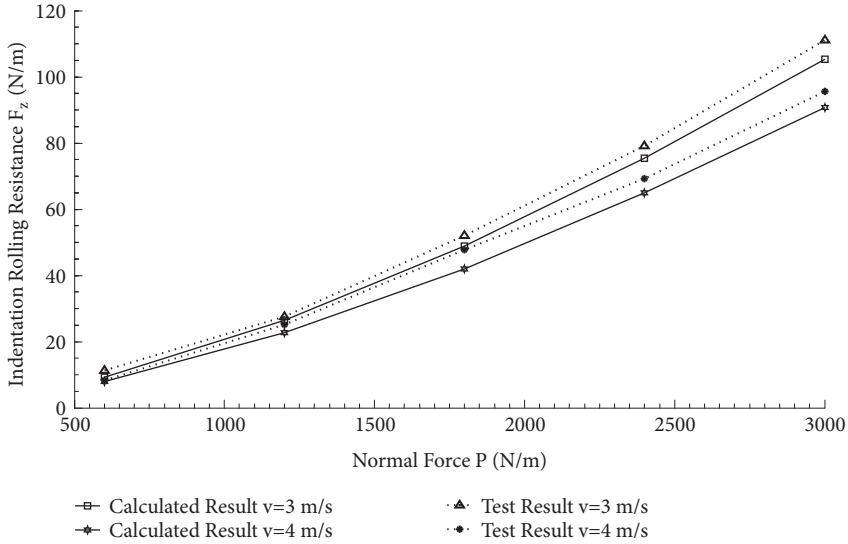

Figure 23: Comparison diagram of theoretical results and experimental results at different normal forces—T=0°C, R=0.0445 m, h=0.006 m.

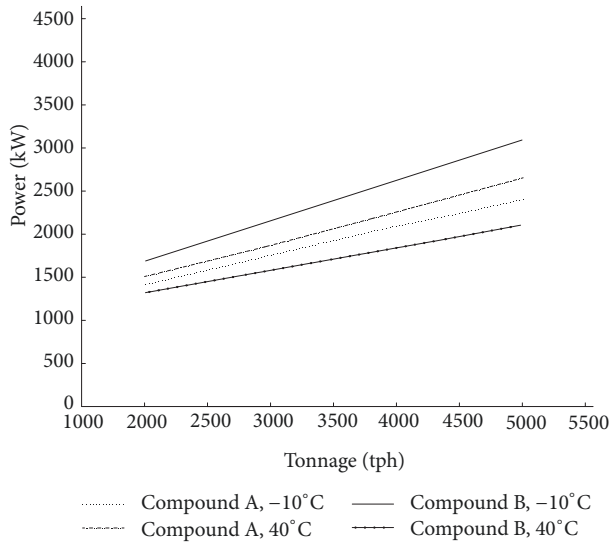

Figure 24: Relationship between conveyor capacity and power of belt conveyor at different temperatures.

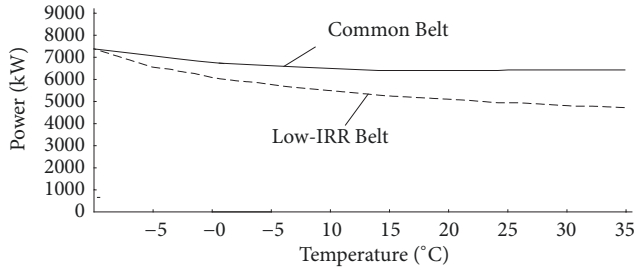

Figure 25: Temperature and power curves.

Therefore, reducing energy consumption by reducing the energy loss of IRR is an effective way to save energy. One of the ways to reduce the IRR is to change the rubber composition of the belt cover effectively. According to the theory and experiment in this paper, the IRR of a kind of covering rubber at a certain temperature can be calculated first and then verified again by the test. A company in China constantly changes the rubber composition of the cover layer to develop a low-IRR conveyor belt. It turns out that the low-IRR conveyor belt can effectively save about 20% of the energy consumption of the entire conveyor system. The power comparison of the two different conveyor belts is shown in Figure 25.

7. Conclusion

In this paper, based on the three-parameter Maxwell solid model, the dynamic tensile test of cylindrical rubber is completed, and the mathematic models of elastic moduli E_2 and E_3 and viscous coefficient η_2 of rubber are obtained by fitting the data. The models directly reflect the influence of temperature on viscoelastic parameters. The cylinder used in the test is made of L-type cover rubber. After that, the mathematical model of the indentation rolling resistance is derived, which is characterized by the belt conveyor parameters, such as idler radius R, the belt speed v, the thickness of cover layer h, and viscoelastic parameters. The ambient temperature affects the IRR by viscoelastic parameters E_2, E_3, and η_2. The normal force P has an influence on IRR indirectly by affecting the contact area length between the conveyor belt and idler. Aiming at the mathematical model, the paper analyzes IRR under the working conditions of any combination of different parameters in detail.

The increase in the idler radius and the belt speed can cause a reduction in the indentation rolling resistance. The IRR increases with the increase of the normal force and the thickness of the cover layer. The effect of temperature on the rolling resistance of the indentation is generally declining,

Table 3: Change range of IRR at different conditions.

Working condition	Change parameter	Change range of IRR
-20°C+3000 N/m+0.0445 m+0.005 m	v : 1 m/s⟶10 m/s	Decrease 71.12%
-20°C+2400 N/m+0.0445 m+1 m/s	h : 0.0015 m⟶0.01 m	Increase 60.53%
3000 N/m+0.0795 m+0.003 m+ 2 m/s	T: -20°C⟶40°C	Decrease 9.78%
-10°C+0.054 m+0.003 m+1 m/s	P: 600 N/m⟶3000 N/m	Increase 90.98%
20°C+1800 N/m+0.003 m+2 m/s	R: 0.038 m⟶0.0795 m	Decrease 30.82%

but the magnitude is small. Under the specific working conditions, the variation amplitude of IRR with different parameters is shown in Table 3.

Although the working conditions are different, we cannot simply compare the percentage in Table 3, but we can still see the general trend. According to the influence of the IRR, the order from large to small is the normal force, the belt speed and the thickness of the cover layer, the idler radius, and the ambient temperature.

In addition, the author's team developed an experimental device for the IRR test system. The device includes an environment control room, which can adjust the working temperature of the indoor belt conveyor through the cooling/heating operation. A series of experiments can be finished with the equipment. At last, the theoretical calculation results are compared with the experimental results. Although the two-part results have certain errors in a certain value, the overall influence trend on the indentation rolling resistance is the same.

In actual engineering, in order to reduce the power consumption of the belt conveyor, the purpose can be achieved by reducing the IRR. Of course, the factors affecting the IRR should be considered comprehensively.

Data Availability

The data used to support the findings of this study are available from the corresponding author upon request.

Conflicts of Interest

The authors declared no potential conflicts of interest with respect to the research, authorship, and/or publication of this article.

Acknowledgments

The authors received the financial support provided by the National Natural Science Foundation Project (51575370), the 2014 Shanxi Province Coal Based Key Scientific and Technological Project (MJ2014-09), the 2014 Shanxi Province Coal Based Key Scientific and Technological Project (MJ2014-02), and the Research Foundation for Returning Scholar in 2016 of Shanxi province (2016-094).

References

[1] H. Lauhoff, "Speed control on belt conveyors - Does it really save energy?" *Bulk Solids Handling*, vol. 25, no. 6, pp. 368–377, 2005.

[2] R. Król, W. Kisielewski, D. Kaszuba, and L. Gładysiewicz, "Testing belt conveyor resistance to motion in underground mine conditions," *International Journal of Mining, Reclamation and Environment*, vol. 31, no. 1, pp. 1–13, 2017.

[3] M. Hager and A. Hintz, "Energy-saving design of belts for long conveyor systems," *Bulk Solids Handling*, vol. 13, no. 4, pp. 749–758, 1993.

[4] Y.-F. Hou and Q.-R. Meng, "Dynamic characteristics of conveyor belts," *Journal of China University of Mining and Technology*, vol. 18, no. 4, pp. 629–633, 2008.

[5] J. Li and X. Pang, "Belt conveyor dynamic characteristics and influential factors," *Shock and Vibration*, vol. 2018, Article ID 8106879, 13 pages, 2018.

[6] G. Chen, X. Zhang, Z. J. Wang, and F. Li, "An enhanced artificial bee colony-based support vector machine for image-based fault detection," *Mathematical Problems in Engineering*, vol. 2015, Article ID 638926, 12 pages, 2015.

[7] S. C. Hunter, "The rolling contact of a rigid cylinder with a viscoelastic half space," *Journal of Applied Mechanics*, vol. 28, no. 4, p. 611, 1961.

[8] F. De S. Lynch, "A finite element method of viscoelastic stress analysis with application to rolling contact problems," *International Journal for Numerical Methods in Engineering*, vol. 1, no. 4, pp. 379–394, 1969.

[9] A. Bazergui and M. L. Meyer, "Embedded strain gages for the measurement of strains in rolling contact - Paper illustrates application of the embedded-strain-gage technique to the measurement of subsurface strains in rolling contact with nonlimiting longitudinal tangential tractions," *Experimental Mechanics*, vol. 8, no. 10, pp. 433–441, 1968.

[10] C. O. Jonkers, "The indentation rolling resistance of belt conveyors: a theoretical approach," *Fördern und Heben*, vol. 30, no. 4, pp. 312–317, 1980.

[11] C. Spaans, "Calculation of the main resistance of belt conveyors," *Bulk Solids Handling*, vol. 11, no. 4, pp. 809-82, 1991.

[12] G. Lodewijks, "Determination of rolling resistance of belt conveyors using rubber data: Fact or fiction?" *Bulk Solids Handling*, vol. 23, no. 6, pp. 384–391, 2003.

[13] T. J. Rudolphi and A. V. Reicks, "Viscoelastic indentation and resistance to motion of conveyor belts using a generalized maxwell model of the backing material," *Rubber Chemistry and Technology*, vol. 79, no. 2, pp. 307–319, 2006.

[14] T. J. Rudolphi and A. V. Reicks, "The importance of non-linear strain consideration in belt conveyor indentation loss," *Bulk Solids Handling*, vol. 32, no. 2, pp. 52–57, 2012.

[15] X. Qiu, "Full two-dimensional model for rolling resistance: Hard cylinder on viscoelastic foundation of finite thickness," *Journal of Engineering Mechanics*, vol. 132, no. 11, pp. 1241–1251, 2006.

[16] X. Qiu and C. Chai, "Estimation of energy loss in conveyor systems due to idler indentation," *Journal of Energy Engineering*, vol. 137, no. 1, pp. 36–43, 2011.

[17] L. Gladysiewica and M. Konieczna, "Theoretical basis for determining rolling resistance of belt conveyors," *Mining Science*, vol. 23, pp. 105–119, 2016.

[18] P. W. Robinson and C. A. Wheeler, "The indentation rolling resistance of spherically profiled idler rolls," *International Journal of Mechanical Sciences*, vol. 106, pp. 363–371, 2016.

[19] C. Wheeler, "Indentation rolling resistance of belt conveyors - A finite element solution," *Bulk Solids Handling*, vol. 26, no. 1, pp. 40–43, 2006.

[20] F. Qiu, Y. Yu, and T. Rudolphi, "Finite element modeling of viscoelastic stress analysis under moving loads," *Proceedings of World Academy of Science Engineering & Technology*, vol. 1, no. 74, pp. 226–233, 2011.

[21] S. Hötte, S. Von Daacke, L. Schulz, L. Overmeyer, and T. Wennekamp, "The way to DIN 22123 - Indentation rolling resistance of conveyor belts," *Bulk Solids Handling*, vol. 32, no. 6, pp. 48–52, 2012.

[22] F. Wang, "Indentation rolling resistance of conveyor belts based on maxwell model," *Advanced Materials Research*, vol. 479-481, pp. 1526–1529, 2012.

[23] J. I. O'Shea, C. A. Wheeler, P. J. Munzenberger et al., "The influence of viscoelastic property measurements on the predicted rolling resistance of belt conveyors," *Journal of Applied Polymer Science*, vol. 131, no. 18, pp. 1–9, 2014.

[24] J. I. O'Shea and C. A. Wheeler, "Dielectric relaxation studies of conveyor belt compounds to determine indentation rolling resistance," *International Journal of Mechanics and Materials in Design*, vol. 13, no. 4, pp. 553–567, 2017.

[25] P. Munzenberger and C. Wheeler, "Laboratory measurement of the indentation rolling resistance of conveyor belts," *Measurement*, vol. 94, pp. 909–918, 2016.

[26] Y. Lu, F. Lin, and Y. Wang, "Investigation on influence of speed on rolling resistance of belt conveyor based on viscoelastic properties," *Journal of Theoretical and Applied Mechanics*, vol. 45, no. 3, pp. 53–68, 2015.

[27] Y. Lu and F. Lin, "A study of indentation rolling resistance to motion of conveyor belts using a generalized Maxwell model of the backing material," *Proceedings of the Institution of Mechanical Engineers, Part J: Journal of Engineering Tribology*, vol. 230, no. 8, pp. 1006–1018, 2016.

[28] L. Yan, "Investigation on indentation rolling resistance of belt conveyor based on Hertz contact theory compared with one-dimensional Winkler foundation," *Advances in Mechanical Engineering*, vol. 10, no. 7, pp. 1–9, 2018.

[29] J. Mao and C. H. Yang, "Theoretical research on indentation resistance to conveyor belt," *Chinese Journal of Applied Mechanics*, vol. 26, no. 3, pp. 461–468, 2009.

[30] H.-Y. Chen, K. Zhang, M.-B. Piao, X. Wang, and E.-D. Li, "Dynamic analysis of indentation rolling resistance of steel cord rubber conveyor belt," *Journal of Mechanical Science and Technology*, vol. 32, no. 9, pp. 4037–4044, 2018.